Optimal sizing of PV/wind/battery Hybrid Renewable Energy System Considering Demand Side Management

Kanwarjit Singh Sandhu and Aeidapu Mahesh

Department of Electrical Engineering, NIT Kurukshetra
kjssandhu@rediffmail.com, mahesh.aeidapu@gmail.com

Abstract: This paper the effect of demand side management (DSM) on the sizing of hybrid PV/wind/battery energy in system has been considered. The pigeon inspired algorithm (PIO) has been used for optimization purpose and additionally an energy filter algorithm has been developed to minimize the fluctuations of power injected into the grid. The levelized cost of energy (LCE) has been taken as the objective function while maintaining the system reliability, healthy charge on the battery as well as the less fluctuations in the power injected into the grid. The simulation has been performed for both actual load and modified load after the DSM has been performed. To verify the results a case study has been considered and the simulations are carried out in MATLAB environment. The results indicate that the DSM considerably reduces the storage requirements and there by reducing the unit cost.

Keywords: Size optimization, Demand side Management, Pigeon inspired optimization

1. Introduction

To meet the increasing day to day load demand, the conventional sources do not seem to be the suitable option and moreover they are rapidly depleting. This serious concern has alarmed a need for a search of alternative, sustainable and clean energy sources for future. The renewable energy sources like solar energy and wind energy have great potential to solve this energy crisis when compared to the other sources. Unlike the conventional sources, the solar and wind sources are widely distributed all around the world, making these resources available irrespective of the place even in the remote locations where lying of transmission lines is difficult. But, the problem with these sources is their intermittent nature. The power from these resources will always vary with respect to the solar radiation and wind speed. Because of this intermittent nature, these sources when used independently are not going to be completely reliable and also less cost effective. A hybrid system comprising of PV and wind sources can be a suitable alternative to improve the reliability as these sources naturally complement each other. To satisfy the load demand and also to store the excess power, battery banks are usually added to the system working in stand-alone mode. In grid connected mode, the grid acts as the source as well as sink in case of power deficiency and excess power availability. The demand side management is one of the key ideas of smart grid which allows the users to manage their load according to the price of power. It comprises of planning, implementation and monitoring of activities of 1 utilities that influence the customer energy consumption. As a result of which the consumer load pattern in going to change depending on the situation. The DSM can be used to achieve various objectives, such as load shifting, peak-shaving, valley filling, flixible load shape, strategic load growth and strategic conversion [1]. Different combinations of the above techniques would make it possible to match the generation and the load profiles closely.

And this would decrease the generation cost and also the load factor can be significantly improved [2]. In general the goal of the DSM is that the users are encouraged to reduce their consumption during peak - hours or to shift the use of appliance to non-peak hours so that the load demand curve is flattened. In few cases instead of flattening, following the generation pattern is more desirable. The peaks in the system appear only for a short duration of time but, the entire system should be designed for the peak demand. The DSM aims to reduce the peak, which reduces the generation and transmission costs drastically and also allows better utilization

Received: December 27th, 2016. Accepted: March 2th, 2018
DOI: 10.15676/ijeei.2018.10.1.6

of assets. In existing system, the peak-shaving serves as the virtual capacity addition also reduces the reserve margins [3].

As far as the optimization is concerned there are several optimization strategies being employed by the researchers for the optimal sizing of stand-alone hybrid renewable energy systems. They are basically single objective optimization strategies and multi-objective optimization strategies in the literature. For single objective optimization the main objective is to minimize the system cost, with reliability and other constraints and for multiobjective optimization the cost and reliability are treated separately. These optimization functions have been solved using iterative techniques [4–8], graphical construction method [9, 10], least squares[11] and evolutionary algorithms like genetic algorithm [12–18], simulated annealing [19], Strength Pareto Algorithm[20], artificial bee swarm algorithm[21] and ant colony optimization[22] and [23, 24] present a review of such optimization studies.

The existing optimization strategies for grid connected systems are based on the stand-alone strategy by taking the grid as a backup source [25, 26]. In [27], an optimization strategy based on multi criteria decision analysis (MCDA) to find out the optimal size by ranking the various alternatives available is presented for grid connected system. GA has been used to minimize the 20 year system cost. Other size optimization in [28] is done using GA, taking the cost as the objective, extra objectives included are the operating reserve capacity, battery discharge/charge rate and cycles, utilization of complementary characteristics. The authors have used a low pass filter to filter the power fluctuations injected into the grid, which have certain disadvantages like dependence on sampling time and unable to reduce the fluctuations effectively. The other smoothing strategies for stand-alone systems have been presented in [29, 30].

The future energy scenario is completely going to be transformed by virtue of the concept ”Smart Grid”. Unlike the traditional grids where the energy flow is unidirectional, but the smart grid supports a bidirectional power flow, that means the user can also generate the power and sell the excess power to the utility companies.

The main aim of the present work is to find out the effect of DSM on the sizing of PV/wind/battery energy system. For this purpose, the load pattern from [31] has been taken before and after DSM. The optimization has been performed for both the cases, one with the actual load and the other with the load from the DSM and the

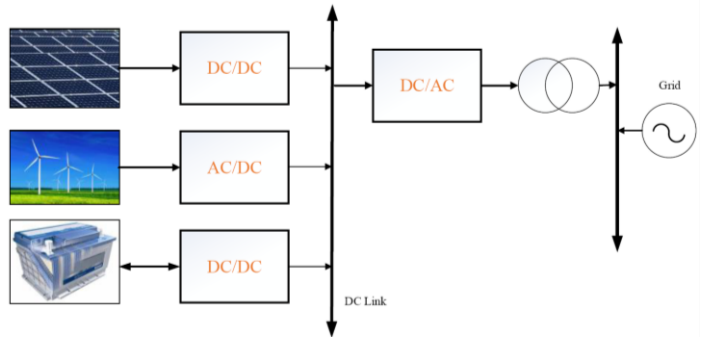

Figure 1. Block diagram representation of hybrid PV-wind-battery system

resulting sizes of both cases are compared for a case study. The optimization strategy includes the following factors i)system reliability ii)full utilization of complementary characteristics, iii)less fluctuations in power injected into the grid, iv)operating reserve. The optimal sizing strategy for sizing Photovoltaic-wind hybrid power system has been formed for satisfying the above mentioned constraints. A novel energy filter algorithm has been developed to reduce the power fluctuations injected into the grid and PIO has been used to optimize the various system components.

The next sections of the paper is organized as follows. Mathematical modeling of the various components of the study have been presented in section 2, Modeling of different parameters used in the optimization is explained in section 3, various costs have been discussed in section 4, New

optimal sizing strategy including the various constraints is presented in section 5 and 6 and in the end results of a case study has been presented to portrait the effectiveness of the proposed algorithm.

2. System Description and Modeling

The block diagram of the hybrid system is as shown in the Figure 1. The PV system is connected to a DC-DC converter to step up the DC level, the wind system is connected to a AC/DC rectifier and finally the batteries are also connected to a DC/DC converter. All these three sources are connected to a common DC bus, then to connect this system to the grid the power is going to be converted to AC by using an inverter and stepped up to the grid level to integrate.

A. PV system modeling

The power output from a PV panel is given by the expression [28]

$$P_{pv} = f_{dr} P_{pv_r} \frac{G}{G_n} [1 - \beta_T (T - T_n)] \quad (1)$$

where, P_{pvr} is the rated power of the PV panel, at the nominal irradiation G_n and nominal temperature T_n. G and T gives the irradiation and the temperature at a particular instant of time and _t gives the temperature co-efficient of power for the silicon material. Here, a factor f_{dr} has been used to consider the effect of dust and icing on the surface of the PV panel.

B. Wind system modeling

The power output at a given wind speed Vm for a wind turbine is expressed as [28]

$$P_{WT} = \begin{cases} 0 & v_w < V_{ci} \text{ or } v_w > V_{co} \\ P_{wt\_r} \frac{v_w - V_{ci}}{v_r - V_{ci}} & V_{ci} < v_w < V_{cr} \\ P_{wt\_r} & V_{cr} < v_w < V_{co} \end{cases} \quad (2)$$

where, V_r is the rated wind speed for the wind turbine, P_{wt} r is the wind turbine rated power output, V_{co} and V_{ci} are the cut-off and cut-in wind velocities for the wind turbine.

C. Battery Modeling

In this work, a battery model which represents the battery as a two-tank system called kinetic battery model (KiBaM) [32] has been used. This model assumes the total energy on the battery as two parts, one is called the available energy and the other is called the bound energy. Figure 2 shows the block diagram of the battery model. Here, the available energy is the energy which is readily available to be supplied to the load, and the bound energy indicates the energy which is chemically bound and not readily available. The bound energy is first converted into the available energy and then only it will be converted to the electrical energy.

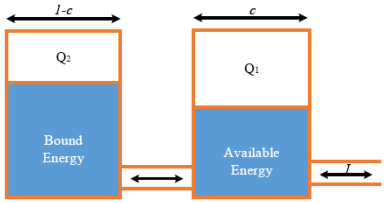

Figure 2. Kinetic Battery Model

If the amount of available energy and the bound energy at a given instant of time are given by Q_1 and Q_2, then the charge levels for the next instant Q_1' and Q_2' are given by,

$$Q = Q_1 + Q_2 \tag{3}$$

$$Q_1^{'} = Q_1 e^{-k\Delta t} + \frac{(Qkc - P_{bs})(1 - e^{-k\Delta t})}{k} + \frac{cP_{bs}(k\Delta t - 1 + e^{-k\Delta t})}{k} \tag{4}$$

$$Q_2^{'} = Q_2 e^{-k\Delta t} + Q(1-c)(1 - e^{-k\Delta t}) + \frac{P_{bs}(c-1)(k\Delta t - 1 + e^{-k\Delta t})}{k} \tag{5}$$

Where, Pbs is the power that is either drawn or supplied to the batteries during the time step Δt, C and K are the capacity ratio and rate constant respectively.

The maximum limit of the charge and discharge power during a particular time step are given by,

$$P_{bs\_dchmax} = \frac{kQ_1 e^{-k\Delta t} + Qkc(1 - e^{-k\Delta t})}{1 - e^{-k\Delta t} + c(k\Delta t - 1 + e^{-k\Delta t})} \tag{6}$$

$$P_{bs\_chmax} = \frac{-kcQ_{max} + kQ_1 e^{-k\Delta t} + Qkc(1 - e^{-k\Delta t})}{1 - e^{-k\Delta t} + c(k\Delta t - 1 + e^{-k\Delta t})} \tag{7}$$

3. Parameters for optimal sizing

A. Loss of power supply probability (LPSP)

To evaluate the reliability of the system, loss of power supply probability (LPSP) is used in this model. LPSP can
be defined as the load that the system is not able to satisfy divided by the total load in the study period[?]. It is given by,

$$LPSP = \sum_{i=1}^{N} \frac{P_L(t_i) - P_{supplied}(t_i)}{\sum^{N} P_L(t_i)} \tag{8}$$

Where, Psupplied(ti) is the total sum of energy supplied by the system at time ti, and N is the total number of hours in the study. In this work N is taken as 8760 i.e. total number of hours in a year. An LPSP value of 0 signifies that the load is completely met at all the times and a value of 1 specifies the load is completely unmet. The allowable value of LPSP is generally taken as 0.05 or 5%.

B. Fluctuations of power injected into the grid

The fluctuations of power injected into the grid are defined by the Median absolute deviation (MAD) and fluctuation rate Dgs, are given by,

$$MAD = median_i\left(|P_{gs}(i) - median_j(P_{gs}(j))|\right) \tag{9}$$

$$D_{gs} = \frac{P_{gs\_max} - P_{gs\_min}}{\Delta t} \tag{10}$$

Where, Pgs max and Pgs min are the maximum and minimum power supplied to the grid in the time interval Δt. MAD gives the robust measure of variability of the uni-variate data. These two parameters, Dgs and MAD can give the short and long term fluctuations of power injected into the grid.

4. Total cost of the system

The total cost of the system includes various costs as shown below.

A. Investment cost

The initial investment cost includes the cost of various equipment, like PV panels, wind turbines and battery bank and different power converters, defined as

$C_{in} = (C_{pv}N_{pv} + C_{wt}N_{wt} + C_{bs}N_{bs})$ x CRF (11)

Where, C_{pv},C_{wt},C_{bs} are the cost of PV panel, cost of wind turbine and cost of battery respectively and N_{pv},N_{wt},N_{bs} are the number of PV panels, number of wind turbines and number of battery banks respectively.

CRF is the capital recovery factor, which is used to convert all the cost to present value, given by

$$CRF = \frac{r(1+r)^{L_p}}{(1+r)^{L_p} - 1} \tag{12}$$

Where, r is the interest rate and Lp is the life time of the project. The investment cost also includes installation cost of the entire system.

The annual investment can be obtained by dividing each of components by it's life time.

$$C_{A\_in} = \left(\frac{C_{pv}N_{pv}}{Y_{pv}} + \frac{C_{wt}N_{wt}}{Y_{wt}} + \frac{C_{bs}N_{bs}}{Y_{bs}}\right) * CRF \tag{13}$$

where, Ypv, Ywt and Ybs are the life time of the PV, wind and the battery bank. Usually the PV panels have a life time of 20-25 years and wind turbines have 15-20 years and the batteries have a life time of 4-5 years.

B. Operation and maintenance cost

Since the fuel is free of cost, the operation and maintenance cost is the major cost for the system. It is given by,

$C_{o\&m} = C_{pvo\&m}t_{pv} + C_{wto\&mtwt} + C_{bso\&m}t_{bs}$ (14)

Where, $C_{pvo\&m}$,$C_{wto\&m}$,$C_{bso\&m}$ are the operating and maintenance cost of PV, wind and battery system per unit time, tpv,twt,tbs are the operating times of PV, wind and battery systems respectively.

C. Cost of power exchange between the grid

Since, the power flow is bidirectional, the cost is also divided into two parts, the cost of power purchased form the

grid (Cgp) and cost of power supplied to the grid (Cgs), and are given by

$C_{gp} = N_{gp} \_ C_p$ (15)

$C_{gs} = N_{gs} \_ C_s$ (16)

Where, Cp, Cg are the cost per unit of power purchased and supplied to the grid and Ngp, Ngs are the total number of units purchased, supplied to the grid respectively.

D. Penalty cost

In stand-alone mode, the unreliability of power can cause a penalty cost, if the LPSP exceeds the specified limit βL. But, in case of grid connected mode in addition to the reliability, the fluctuations in the power also going to cause the penalty when the fluctuations exceed a specified limit βg. So, the penalty cost is given by the expression

$$C_{pc} = C_{pc_1}(LPSP - \beta_L)\sum_{i=1}^{N} P_L(t_i) + C_{pc_2}\frac{D_{gs} - \beta_g}{\beta_g} * 100, \text{if}(LPSP > \beta_L)\text{and}(D_{gs} > \beta_g) \tag{17}$$

Where, Cpc1 is the penalty cost for the shortage of supply ($/kWh) and Cpc2 is the cost for fluctuation in the

supply($/%).

E. Total cost of the system

The total cost of the system comprises of all the costs said above, added with a replacement cost (Cr) which takes care of any components replaced due to failure or the aging. This (Cr), is usually accounted if any component's life span is less than the project life time.

Now, the total cost Ctotal can be expressed as

$C_{A\ total} = C_{A\ in} + C_{o\&m} + C_{gp} - C_{gs} + C_r$ (18)

F. Levelized cost of energy (LCE)

The LCE is expressed by the total cost of the hybrid system divided by the total energy generated by the system.

Given by,

$$LCE = \frac{C_{A\_total}}{E_{total}} \tag{19}$$

Where, Etotal gives the total energy supplied by all three sources together. This LCE can be used as a measure to optimize the system economically. The combination with the least value of LCE can be the most attractive solution, provided it satisfies all the other requirements.

5. Constraints for optimization

A. Reliability constraint

For providing the reliable supply to the load, the system has to satisfy the reliability constraint, given by

$LPSP \leq \beta_g$ (20)

Where, _L is the tolerance limit of the reliability of the system.

B. Fluctuations of power injected into the grid

As the fluctuations are directly going to lead for the penalty cost based on equation (17), the Dgs must be limited to the allowable limits. Therefore, the constraint for this is given by

$D_{gs} \leq \beta_g$ (21)

According to [28], the maximum allowed fluctuation in the power is the 33% of the installed capacity within 10 minutes. And also MAD must also be as small as possible to inject less fluctuent power into the grid.

C. Battery constraints

As the batteries are the components with the least life span in the system, they need to be given most attention. In this method, the battery state of charge (SOC) is maintained within the minimum (SOCmin) and maximum (SOCmax) limits to ensure that the battery is neither completely discharged and nor fully charged at any point of time. This will improve the battery life time. And the charge (Pbs ch) and discharge power (Pbs dch) at any point of time are to be kept at within the maximum charge and discharge power limits to regulate the flow of charge to the battery. And also the charge (Pbs ch) and discharge currents(Ibs dch) are also to be maintained within the limits. The constraints are given by

$SOC_{min} \leq SOC \leq SOC_{max}$ (22)

$0 \leq P_{bs\ ch} \leq P_{bs\ chmax}$ (23)

$0 \leq P_{bs\ dch} \leq P_{bs\ dchmax}$ (24)

D. Operating reserve

Operating reserve is the energy which is available in excess to supply to the instant increase in the load. Given by

$$P_{ic} = (1 + \mu\%) \sum_{i=1}^{N} P_L(t) \tag{25}$$

Where, Pic is the total installed capacity of the system and _ is the percentage ratio of the operating reserve. An operating reserve of 10% is generally taken while planning for a distributed generation.

E. Objective function formulation

In the present work, the main objective function considered is the cost of the system. It is defined by

$$minf = min(LCE) \quad (26)$$

That means the combination with the minimum levelized cost, while satisfying the constraints (20) - (25) will be the final optimal solution.

6. Optimal sizing of the system

A. Energy management in grid connected system

In the grid connected system, two operating conditions usually arise, one is when the power produced is not sufficient to meet the load demand, and the other is the power generated is more than the load demand. In the first case the rest of the power to meet the load is drawn from the grid. It can be represented as,

$$P_L(t) = P_{pv}(t) + P_{wt}(t) + P_{bs\_dch}(t) + P_{gp}(t) \quad (27)$$

Here, $P_{gp}(t)$ is the power purchased form the grid. Similarly, the second scenario can be expressed as

$$P_{gs}(t) = P_{pv}(t) + P_{wt}(t) - P_{bs\_ch}(t) - PL(t) \quad (28)$$

Here, $P_{gs}(t)$ is the power supplied to the grid at an instant of time. Clearly, in the second case, the priority is always given to the batteries over supplying to the grid, as they are going to play a key role in keeping the system reliable.

7. Pigeon Inspired Optimization

The PIO is also a swarm based algorithm, which has been developed by the natural homing behavior of pigeons. Due to this special ability, these pigeons have been widely used in World War II for communication. The pigeons can track the way back home by depending on three factors; the sun, the magnetic field of earth and the landmarks in the way. This behaviour has been modeled as an algorithm, which can be used to solve optimization problems.

The main operator used int PIO are the map & compass operator and the landmark operator. Initially in a ddimensional space, random pigeons are generated, each will have an initial velocity and the position. Then for each pigeon, the fitness value is calculated and the best of all is called as the Gbest. By using the best pigeon velocity and position, the rest of pigeons are going to adjust their own map & compass operators, which is give by,

$$V_i(t) = V_i(t - 1)e^{-Rt} + rand.(G_{best} - X_i(t - 1)) \quad (29)$$

$$X_i(t) = X_i(t - 1) + V_i(t) \quad (30)$$

where, R denotes the map & compass factor, rand is a random number generated between 0 and 1.

The landmark operator is used to improve the convergence speed after certain number of iterations (75% iterations), in which the total number of pigeons is divided into half every time, and the pigeons which are away from the center are set to follow the other half of pigeons which are near to the center. The implementation is given by

$$N_P(t) = \frac{N_P(t-1)}{2} \quad (31)$$

$$X_c(t) = \frac{\sum X_i(t).fit(X_i(t))}{N_P \sum fit(X_i(t))} \quad (32)$$

and the position updation rule is given by

$$X_i(t) = X_i(t - 1) + rand(X_c(t) - X_i(t - 1)) \quad (33)$$

The strategy used in this PIO is almost similar to the PSO algorithm, but the PIO has been found to have very fast convergence rate, when compared to the other evolutionary algorithms.

A. Optimization strategy

A.1. Proposed strategy with energy filter

In order to overcome the shortcomings of the energy filter discussed in the previous section, a novel energy filtering algorithm has been proposed in this work. The flow chart of the algorithm has been shown in the Figure 4.

This algorithm works on the basis of dynamic averaging. For and instant value Pgs(k), a dynamic average Pgs avg(k) will be calculated using equation (34).

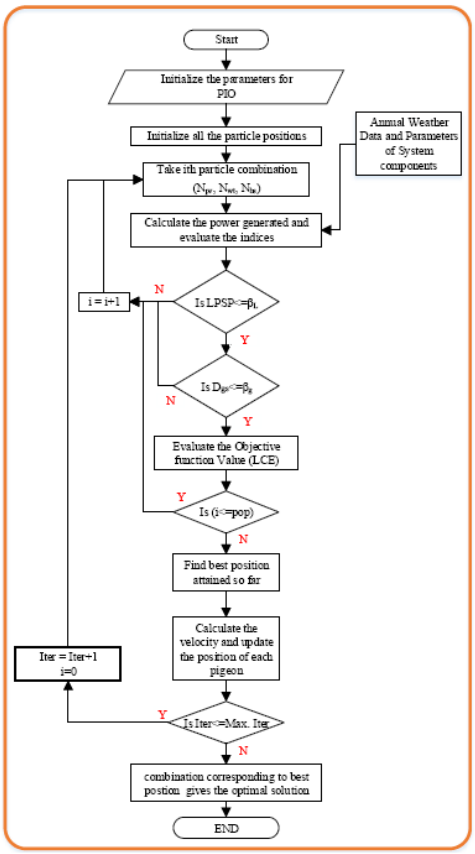

Figure 3. Proposed optimization strategy

$$P_{gs\_avg}(k) = \frac{\sum_{i=1}^{k} P_{gs}(i)}{k} \quad (34)$$

Then, the deviation (Dev) of the present value with respect to the average Pgs avg(k) is calculated using

$$Dev = (P_{gs\_avg}(k) - P_{gs}(k)) \times EFC \quad (35)$$

where, EFC is the Co-efficient of energy filter. Here, by varying the EFC, we can set the proportion of deviation from the average which is to be considered for filtering.

Then, the updated value of $P_{gs}(k)$ is calculated using the following equation,

$$P_{gs}(k) = \begin{cases} P_{gs}(k) + (N_{bs} * P_{bs\_dch}(k)), & if(avg - P_{gs}(k)) > Dev \\ P_{gs}(k) - (N_{bs} * P_{bs\_ch}(k)), & if(avg - P_{gs}(k)) < -Dev \\ P_{gs}(k), & \text{any other value} \end{cases} \quad (36)$$

After calculating the updated value of Pgs(k), it will be adjusted such that the power that is to be supplied to or from the batteries is within the maximum limits.

The proposed energy filter algorithm gives the following advantages
1. The dynamic averaging is more effective in reducing the fluctuations.
2. The maximum and minimum levels of fluctuations can be chosen according the situation.
3. There is no dependency of output on sample time, as we are going to sample for each hour.
4. Here, the positive and negative portions of deviations can be controlled independently, this is one of the greatest advantage in case the power fluctuations are more in any one of the regions.

The only limitation in this algorithm is that, in the case of negative deviation, in order to increase the value of $P_{gs}(k)$ towards the dynamic average, batteries are to be discharged slightly. To avoid this problem, instead of supplying whole battery power available at that instant, we can supply less amount of power to reduce the battery discharging. This is not going to effect the performance of the proposed method, since the number of negative deviation instances are relatively very less compared to positive deviation instances.

8. Case study and Results

For this case study, the location chosen was Logan International Airport, Boston, MA, USA(42.360 N,71.010 W). The meteorological data patterns were taken from the typical meteorological year (TMY3 [?]), and are as shown in the Figure 5. The load data has been taken from [31] and as shown in the Figure 6. Figure 6(a) shows the load

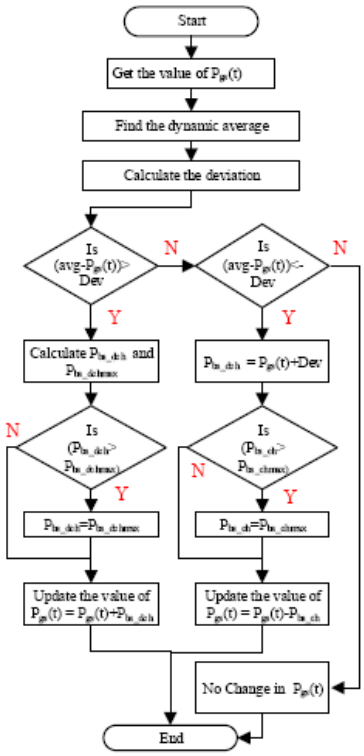

Figure 4: Proposed energy filter algorithm

demand before applying the DSM strategy and the same load has been remodeled by using the DSM is as shown in the Figure 6(b). It can be clearly seen from the Figures that the peak demand has been considerbly reduced and it has been moved on to the non peak hours.

The specifications and the various costs of the PV panel and wind turbine and battery bank used have been given in Table 1. The variables used for calculation of PV output _t is taken as -0.48 and fdr is taken as 85 %. Assuming that the PV is operating at MPP condition, the factor fMPP is taken as 1. The maximum charge on the battery Qmax is taken as 720 Ah and the parameters k & c are taken as 0.34 and 0.98 respectively. The simulations for both the load patterns are carried out and the results are as shown in Table 2. The system size in case of wihout demand side management is Npv= 5120, Nwt = 18, Nbs = 3606. And when the simulation has been carried out with the modified load using DMS the result comes out to be Npv= 4916, Nwt = 20, Nbs = 2674. The LPSP in both the cases is limited to 0.05. From these Figures it can be clearly seen that there is a considerable over-sizing of the hybrid system when the actual load demand is considered. The number of PV panels and batteries required are reduced in the second case and wind being more cost-effective alternative to PV and batteries has been increased. And as a result the cost per unit of electricity CPU ($/kWH) is reduced from

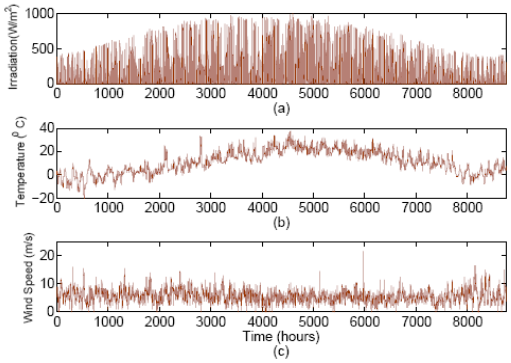

Figure 5. Meteorological data patterns
(a) Hourly solar irradiation (b) Hourly temperature (c) Hourly wind speed

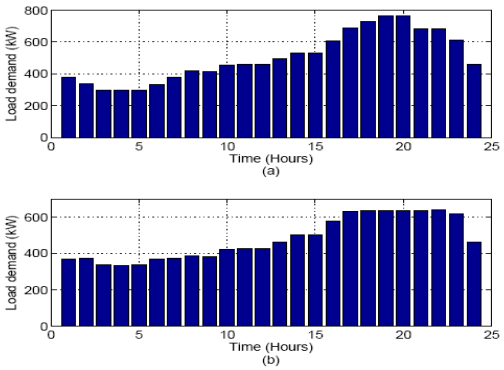

Figure 6. Daily load demand (a) Actual (b) After applying DMS

Table 1. Parameters of system components

(a) PV panel : SANYO HIT Power 200

Parameter	Value
Maximum Power	200 Watts
Open circuit voltage	68.7 V
Short circuit current	3.83 A
Voltage at MPP	55.8 V
Current at MPP	3.59 A
Efficiency at STC	17.2
Slope (Fixed slope)	40.98^{0}
Cost per panel (C_{pv})	$ 420
O & M cost ($C_{pv_{o\&m}}$)	$ 15 /kW

(b) Wind turbine: PGE 35 kW

Parameter	Value
Rated power	35 kW
Cut-in wind speed	3 m/s
Cut-out wind speed	25 m/s
Hub height	24 m
Rated power wind speed	11 m/s
Rotor diameter	19.2 m
Blade length	9 m
Cost per turbine (C_{wt})	$ 25000
O & M cost ($C_{wt_{o\&m}}$)	$ 30 /kW

(c) Battery : Hoppecke 6OPzS 600

Parameter	Value
Rated capacity	600 Ah
Rated voltage	2 V
Round trip efficiency	85 %
Max. Ch./disch. rate	0.5 A/Ah
Max. ch/disch. current	100 A,75 A
Self-discharge rate	1%
Cost per battery (C_{bs})	$ 150
O & M cost ($C_{bs_{o\&m}}$)	$ 20/kAh

0.3902 to 0.3449.

One of the major advantage obtained by using the DSM is that it reduces the peak load demand which has to be supplied by the batteries most of the time. The batteries are the most costliest and the least life span devices in the system and also require very frequent maintenance. By reducing the number of batteries all of these problems can be reduced to a certain extent.

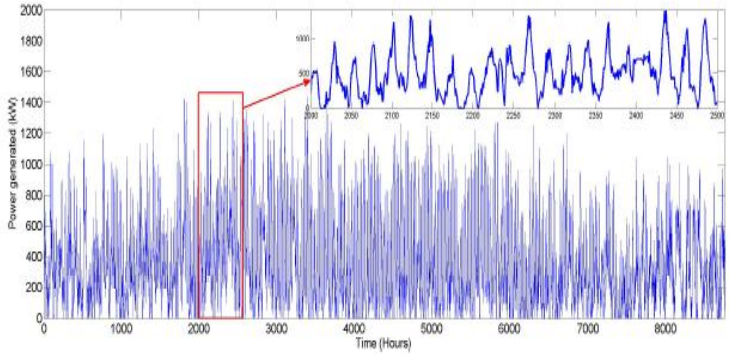

Figure 7. Power generated by the hybrid system

The maximum allowable fluctuation rate _g for the power injected into the grid should not exceed 33% of total installed capacity in 10 minutes according to [28]. Considering the fact that in worst case there will be only one source is delivering the power and the _g value can be taken as

β_g = min (33% _ PV IC; 33% _WT IC) (37)

where, PV IC is the PV installed capacity and ET IC is the wind installed capacity. If the fluctuation rate is less than this value, then it will satisfy the requirement in any case. The allowed fluctuation rate for both of the cases is 207.9 kW and 231 kW respectively as shown in the Table 2.

The energy filter algorithm has been used for reduction in fluctuation of power injected into the grid. The Figure. 8 shows the power injected into the grid with and without energy filter algorithm employed. From the Figure it can be clearly seen that the fluctuations in the power

injected into the grid are considerably reduced and the fluctuation rate after employing the energy filter is 89.67 kW and 86.34 kW for both without and with DSM strategies, which indicates the energy filter algorithm is satisfactorily reducing the fluctuations in the power.

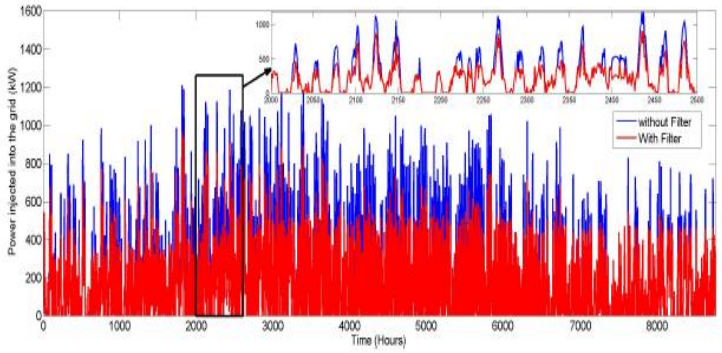

Figure 8. Power supplied to the grid

Figure 9 shows the power drawn or supplied by the battery at each hour. Here a positive value of power indicates the battery is discharging and a negative power indicates the battery is charging. The Figure 10 shows the battery SOC over the entire study period, and from the result it can be seen that the it is always maintained within the acceptable limits.

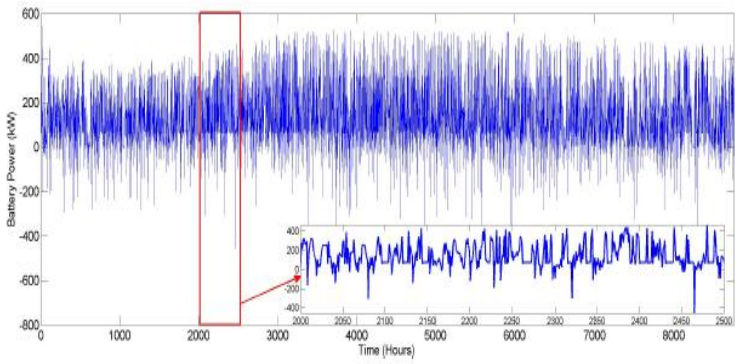

Figure 9. Battery power

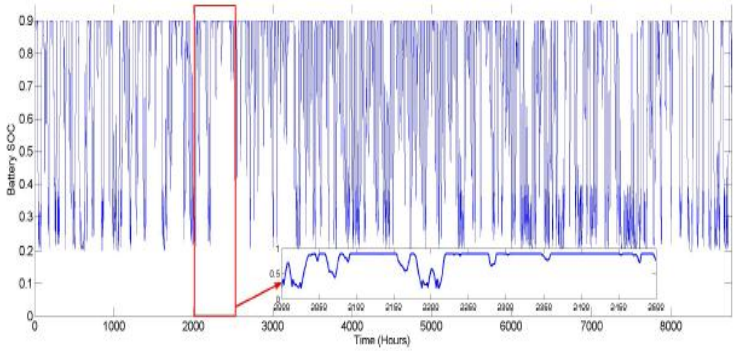

Figure 10. Battery SOC

Table 2. Results with and without DSM

Parameter	Without DSM	With DSM
$(N_{pv}/N_{wt}/N_{bs})$	(5120 / 18 / 3606)	(4916 / 20 / 2674)
C_{PU} (\$)	0.3902	0.3449
C_A (\$)	$8.5998X10^5$	$7.229X10^5$
LPSP	0.05	0.0498
D_{gs} $(kW/\Delta t)$	89.67	86.34
β_g (kW)	207.9	231
MAD (kW)	135.32	144.76

From all the results discussed, it can be seen that the same amount of load can be supplied at a lower cost with reduced number of distributed generation sources.

9. Conclusion

In this paper an attempt has been made to see the effect of DMS on the sizing of a PV/wind/battery hybrid energy system using an energy filter. The mathematical modeling of all the sources and the proposed strategy has been explained in detail. The simulation study has been performed for the two load patterns i.e. actual load and the modified load by using DSM. From the results it can be concluded that the DSM has the positive effect on sizing of the system, which includes huge reduction in the number of energy storage elements required thus resulting in the less cost per unit of electricity.

10. References

[1]. C. W. Gellings. The concept of demand-side management for electric utilities. *Proceedings of the IEEE*, 73(10):1468–1470, Oct 1985.

[2]. Goran Strbac. Demand side management: Benefits and challenges. Energy Policy, 36(12):4419 – 4426, 2008.

[3]. Linas Gelazanskas and Kelum A.A. Gamage. Demand side management in smart grid: A review and proposals for future direction. *Sustainable Cities and Society*, 11:22 – 30, 2014.

[4]. Hocine Belmili, Mourad Haddadi, Seddik Bacha, Mohamed Fayal Almi, and Boualem Bendib. Sizing standalone photovoltaicwind hybrid system: Techno-economic analysis and optimization. Ren. and Sust. Ener. Rev., 30(0):821 – 832, 2014.

[5]. Carlos Eduardo Camargo Nogueira, Magno Luiz Vidotto, Rosana Krauss Niedzialkoski, Samuel Nelson Melegari de Souza, Luiz Incio Chaves, Thiago Edwiges, Darlisson Bentes dos Santos, and IvanWerncke. *Sizing and simulation of a photovoltaic-wind energy system using batteries*, applied for a small rural property located in the south of brazil. Ren. and Sust. Ener. Rev., 29(0):151 – 157, 2014.

[6]. Amos Madhlopa, Debbie Sparks, Samantha Keen, Mascha Moorlach, Pieter Krog, and Thuli Dlamini. Optimization of a pvwind hybrid system under limited water resources. *Ren. and Sust. Ener. Rev*., 47(0):324 – 331, 2015.

[7]. W.D. Kellogg, M.H. Nehrir, G. Venkataramanan, and V. Gerez. Generation unit sizing and cost analysis for stand-alone wind, photovoltaic, and hybrid wind/pv systems. *IEEE Trans. on Ener. Conv*., 13(1):70–75, Mar 1998.

[8]. A. Kaabeche, M. Belhamel, and R. Ibtiouen. Sizing optimization of grid-independent hybrid photovoltaic/wind power generation system. Energy, 36(2):1214 – 1222, 2011.

[9]. Tomas Markvart. Sizing of hybrid photovoltaic-wind energy systems. *Solar Energy*, 57(4):277 – 281, 1996.

[10]. B.S. Borowy and Z.M. Salameh. Methodology for optimally sizing the combination of a battery bank and pv array in a wind/pv hybrid system. *IEEE Trans. on Ener. Conv*., 11(2):367–375, Jun 1996.

[11]. Optimum photovoltaic array size for a hybrid wind/pv system. *IEEE Trans. on Ener. Conv*., 9(3):482–488, Sep 1994.

[12]. Bo Zhao, Xuesong Zhang, Peng Li, Ke Wang, Meidong Xue, and Caisheng Wang. Optimal sizing, operating strategy and operational experience of a stand-alone microgrid on dongfushan island. *Appl. Ener*., 113(0):1656 – 1666, 2014.
[13]. Wanxing Sheng, Ke yan Liu, Xiaoli Meng, Xueshun Ye, and Yongmei Liu. Research and practice on typical modes and optimal allocation method for pv-wind-es in microgrid. *Electric Power Systems Research*, 120(0):242 – 255, 2015.
[14]. Mohammad Ali Yazdanpanah Jahromi, Said Farahat, and Seyed Masoud Barakati. Optimal size and cost analysis of stand-alone hybrid wind/photovoltaic power-generation systems. Civil Engg. and Envi. *Systems*, 31(4):283–303, 2014.
[15]. A. Arabali, M. Ghofrani, M. Etezadi-Amoli, M.S. Fadali, and Y. Baghzouz. Genetic-algorithm-based optimization approach for energy management. *IEEE Trans. on Pow. Del*., 28(1):162–170, Jan 2013.
[16]. M. Alsayed, M. Cacciato, G. Scarcella, and G. Scelba. Multicriteria optimal sizing of photovoltaic-wind turbine grid connected systems. *IEEE Trans. on Ener. Conv*., 28(2):370–379, June 2013.
[17]. D. Abbes, A. Martinez, and G. Champenois. Eco-design optimisation of an autonomous hybrid wind photovoltaic system with battery storage. *Renewable Power Generation, IET*, 6(5):358–371, Sept 2012.
[18]. Eftichios Koutroulis, Dionissia Kolokotsa, Antonis Potirakis, and Kostas Kalaitzakis. Methodology for optimal sizing of stand-alone photovoltaic/wind-generator systems using genetic algorithms. *Solar Energy*, 80(9):1072 – 1088, 2006.
[19]. Orhan Ekren and Banu Y. Ekren. Size optimization of a pv/wind hybrid energy conversion system with battery storage using simulated annealing. Appl. Ener., 87(2):592 – 598, 2010.
[20]. S. Diaf, G. Notton, M. Belhamel, M. Haddadi, and A. Louche. Design and techno-economical optimization for hybrid pv/wind system under various meteorological conditions. *Appl. Ener*., 85(10):968 – 987, 2008.
[21]. Akbar Maleki and Alireza Askarzadeh. Artificial bee swarm optimization for optimum sizing of a standalone pv/wt/fc hybrid system considering lpsp concept. Solar Energy, 107(0):227 – 235, 2014.
[22]. Abdolvahhab Fetanat and Ehsan Khorasaninejad. Size optimization for hybrid photovoltaicwind energy system using ant colony optimization for continuous domains based integer programming. *Applied Soft Computing*, 31(0):196 – 209, 2015.
[23]. Arturo Alarcon-Rodriguez, Graham Ault, and Stuart Galloway. Multi-objective planning of distributed energy resources: A review of the state-of-the-art. *Renewable and Sustainable Energy Reviews*, 14(5):1353 – 1366, 2010.
[24]. Aeidapu Mahesh and Kanwarjit Singh Sandhu. Hybrid wind/photovoltaic system developments: Critical review and findings. *Renewable and Sustainable Energy Reviews*, 0(0):Article in Press, 2015.
[25]. R. Chedid and S. Rahman. Unit sizing and control of hybrid wind-solar power systems. Energy Conversion, IEEE Transactions on, 12(1):79–85, Mar 1997.
[26]. R. Chedid, H. Akiki, and S. Rahman. A decision support technique for the design of hybrid solar-wind power systems. Energy Conversion, *IEEE Transactions on*, 13(1):76–83, Mar 1998.
[27]. M. Alsayed, M. Cacciato, G. Scarcella, and G. Scelba. Multicriteria optimal sizing of photovoltaic-wind turbine grid connected systems. Energy Conversion, *IEEE Transactions* on, 28(2):370–379, June 2013.
[28]. Lin Xu, Xinbo Ruan, Chengxiong Mao, Buhan Zhang, and Yi Luo. An improved optimal sizing method for wind-solar-battery hybrid power system. *IEEE Trans. on Sust. Ener*., 4(3):774–785, July 2013.
[29]. W.A. Omran, M. Kazerani, and M.M.A. Salama. Investigation of methods for reduction of power fluctuations generated from large grid-connected photovoltaic systems. Energy Conversion, *IEEE Transactions on*, 26(1):318–327, March 2011.

[30]. Manoj Datta, Tomonobu Senjyu, Atsushi Yona, and Toshihisa Funabashi. A fuzzy based method for leveling output power fluctuations of photovoltaic-diesel hybrid power system. *Renewable Energy*, 36(6):1693 – 1703, 2011.
[31]. I. Atzeni, L. G. Ordez, G. Scutari, D. P. Palomar, and J. R. Fonollosa. Noncooperative and cooperative optimization of distributed energy generation and storage in the demand-side of the smart grid. *IEEE Transactions on Signal Processing*, 61(10):2454–2472, 2013.
[32]. James F. Manwell and Jon G. McGowan. Lead acid battery storage model for hybrid energy systems. *Solar Energy*, 50(5):399 – 405, 1993.

Kanwarjit Singh Sandhu was born on December 21, 1957. He received the B.Sc.Eng. (electrical), M.Sc. (electrical), and Ph.D. (electrical machines) degrees from Regional Engineering College, Kurukshetra University, Kurukshetra, India, in 1981, 1985, and 2001, respectively. Currently, he is a Professor in the Electrical Engineering Department and also Dean (Academic), National Institute of Technology, Kurukshetra. He has many publications in the area of induction generators. His areas of interest include electrical machines, wind energy conversion, and power systems.

Aeidapu Mahesh was born on October 16, 1989. He received degree of Master of Engineering in Electrical Engineering from PEC University of Technology Chandigarh, India and Batchelor of Technology from JNTU Hyderabad in 2012 and 2010. He is currently working as an Assistant Professor in Electrical Engineering Department of National Institute of Technology Kurukshetra, Haryana, India. His areas of intrest include Hybrid renewable energy systems and Power electronics.